ASM Sc. J., 12, Special Issue 5, 2019 for ICoAIMS2019, 98-106

Stress Intensity Factor for a Thermally Insulated Crack in Bonded Dissimilar Materials

K.B. Hamzah[1,4], N.M.A. Nik Long [1,2*], N. Senu[1,2] and Z.K. Eshkuvatov[3]

[1]*Laboratory of Computational Sciences and Mathematical Physics, Institute for Mathematical Research, Universiti Putra Malaysia, 43400 Serdang, Selangor, Malaysia*

[2]*Mathematics Department, Faculty of Science, Universiti Putra Malaysia, 43400 Serdang, Selangor, Malaysia*

[3]*Faculty of Science and Technology, Universiti Sains Islam Malaysia, 71800 Negeri Sembilan, Malaysia*

[4]*Fakulti Teknologi Kejuruteraan Mekanikal dan Pembuatan, Universiti Teknikal Malaysia Melaka, Hang Tuah Jaya, 76100 Durian Tunggal, Melaka, Malaysia*

The modified complex variable function method with the continuity conditions of the resultant force, displacement and heat conduction functions are used to formulate the hypersingular integral equation (HSIE) for a thermally insulated circular arc crack or a thermally insulated inclined crack in the upper part of bonded dissimilar materials subjected to remote stress. The HSIE is solved numerically for the unknown crack opening displacement function and the known traction along the crack as the right hand term using the appropriate quadrature formulas. Numerical results showed the behavior of the nondimensional stress intensity factor (SIF) at all crack tips. The nondimensional SIF depends on the crack geometries, the distance between crack and the boundary, the elastic constants ratio, the heat conductivity ratio and the thermal expansion coefficients ratio.

Keywords: stress intensity factor; thermally insulated crack; bonded dissimilar materials; modified complex variable; hypersingular integral equation

I. INTRODUCTION

The strength and life cycles of the engineering structure can be effected by emergence of the crack and this situation makes more worsen when the structures are exposed to the thermal. This phenomenon has interested many researchers to investigate the behaviour of stress intensity factors (SIF), which control the stability behaviour of bodies or materials containing cracks or flaws, for the thermoelastic crack problems in an infinite plane (Chen & Hasebe, 2003; Zhong *et al*., 2018), half plane (Jin & Noda, 1993; Li *et al*., 2015) and bonded dissimilar materials (Chao & Shen, 1995; Shevchuk, 2017; Mishra & Das, 2018; Zhou & Kim, 2016; Choi, 2016; Ding & Li, 2015) subjected to remote stress.

The singular integral equations was derived and solved numerically by using the appropriate interpolation formulas for two dimensional thermoelastic crack problems in bonded dissimilar materials (Chao & Shen, 1995). The nondimensional SIF for an undercoat crack perpendicular to the interface of multilayer materials subjected to convective thermal loading were formulated into the system of singular integral equations (Shevchuk, 2017). The nondimensional SIF at the crack tips of the interface crack in bonded thermo-elastic half planes subjected to a uniform heat flux were calculated using the Fredholm integral equations (Mishra & Das, 2018). A system of singular integral equations was derived and solved numerically by using collocation methods for thermally insulated interface crack in functionally graded interlayer materials (Zhou & Kim, 2016). The Mode III nondimensional SIF for the edge interfacial cracks in bonded dissimilar materials were calculated using a system of singular integral equations (Choi, 2016). The thermal SIF and strain energy density for a insulated interface crack in nonhomogeneous structural materials under uniform heat flow was calculated reducing the Fourier transform to the singular integral equations (Ding & Li, 2015).

*Corresponding author's e-mail: nmasri@upm.edu.my

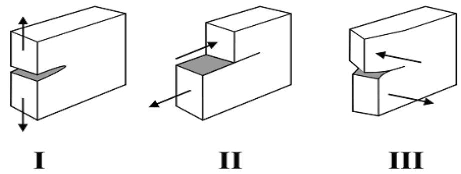

Figure 1. Three types of modes in fracture mechanics

There are three types of modes in fracture mechanics such as tensile opening (Mode I), in plane shear (Mode II) and out of plane tearing (Mode III) as shows in Figure 1 (Shields *et al.*, 1992). The Mode I corresponds to normal separation of the crack faces under the action of tensile stresses. The Mode II is the shear stress acting parallel to the crack faces and perpendicular to the crack front. Whereas the Mode III is a shear stress acting parallel to the crack faces and parallel to the crack front.

The aim of this paper is to investigate the behavior of nondimensional SIF for a thermally insulated circular arc crack or a thermally insulated inclined crack in the upper part of bonded dissimilar materials subjected to the remote shear stress $\sigma_{x_1} = \sigma_{x_2} = p$.

II. MATHEMATICAL FORMULATION

The complex potentials for heat conduction problem introduced by Muskhelishvili (1953) is expressed as

$$\omega(z) = T(x,y) + iQ(x,y) \tag{1}$$

where $T(x,y) = \mathrm{Re}\left[\omega(z)\right]$ is temperature distribution, $Q(x,y) = -k\,\mathrm{Im}\left[\omega(z)\right]$ is resultant heat flux function and k stands for the heat conductivity. Generally the stress components $\left(\sigma_x, \sigma_y, \sigma_{xy}\right)$, the resultant force function (*X*, *Y*), and the displacements (*u*, *v*) for thermally insulated crack in an infinite plane are expressed in terms of three complex potential functions $\phi(z)$, $\psi(z)$ and $\omega(z)$ as follows

$$\sigma_y - \sigma_x + 2i\sigma_{xy} = 2\left[\bar{z}\phi''(z) + \psi'(z)\right] \tag{2}$$

$$f = -Y + iX = \phi(z) = z\overline{\phi'(z)} + \overline{\psi(z)} \tag{3}$$

$$2G(u+iv) = \kappa\phi(z) - z\overline{\phi'(z)} - \overline{\psi(z)} + (1+\kappa)G\beta\int\omega(z)dz \tag{4}$$

where $z = x + iy$ denotes complex variable, G is shear modulus of elasticity, $\kappa = 3-4v$ and $\beta = \left((1+v)\mu\right)/\left(2(1-v)\right)$ for plane strain, $\kappa = (3-v)/(1+v)$ and $\beta = (1+v)\mu/2$ for plane stress, v is Poisson's ratio and μ is the thermal expansion coefficient. A derivative in a specified direction of Eqn. (3) with respect to *z*, yields the normal (*N*) and tangential (*T*) components of traction along the segment $\overline{z, z+dz}$, which is defined as follows

$$\frac{d}{dz}\{f\} = \phi'(z) + \overline{\phi'(z)} + \frac{d\bar{z}}{dz}\left[z\overline{\phi''(z)} + \overline{\psi'(z)}\right] = N + iT. \tag{5}$$

According to Nik Long and Eshkuvatov (2009) and Chen *et al.* (2003), complex potentials for the crack *L* in an infinite thermoelastic modeled by the distribution of crack opening displacement (COD) function, $g(t)$, and the temperature jump along the crack faces, $\gamma(t)$, can be expressed as

$$\phi_{1p}(z) = \frac{1}{2\pi}\int_L \frac{g(t)dt}{t-z} \tag{6}$$

$$\psi_{1p} = \frac{1}{2\pi}\int_L \frac{\overline{g(t)}dt}{t-z} + \frac{1}{2\pi}\int_L g(t)\left[\frac{d\bar{t}}{t-z} - \frac{\bar{t}dt}{(t-z)^2}\right] \tag{7}$$

$$\omega_{1p}(z) = \frac{1}{i\pi}\int_L \frac{\gamma(t)dt}{t-z} \tag{8}$$

where $g(t)$ is defined by

$$g(t) = \frac{2G}{i(\kappa+1)}\left[\left(u(t)+iv(t)\right)^+ - \left(u(t)+iv(t)\right)^-\right], t\in L \tag{9}$$

$\left(u(t)+iv(t)\right)^+$ and $\left(u(t)+iv(t)\right)^-$ denote the displacements at point *t* of the upper and lower crack faces, respectively. Substituting Eqns. (4), (6), (7) and (8) into dislocation distribution $g'(t)$, yields

$$g'(t) = g(t) - 2i\beta\gamma(t). \tag{10}$$

The single-valuedness condition for the displacement

$$\int_L g'(t)dt = 0. \tag{11}$$

Apply Eqn. (11) into (10), yields

$$\int_L \gamma(t)dt = \frac{-i}{2\beta}\int_L g(t)dt. \tag{12}$$

Substituting Eqn. (12) into (8) to represent the complex potential of the temperature jump in terms of COD as

$$\omega_{1p}(z) = -\frac{1}{2\pi\beta}\int_L \frac{g(t)dt}{t-z}. \tag{13}$$

The condition for the stress components in the upper, ε_{x_1} , and lower parts, ε_{x_2} , of bonded dissimilar materials by consider only the shear stress and all other stresses do not exist, then the stress component is reduced to

$$\varepsilon_{x_1} = \varepsilon_{x_2}$$
$$\frac{1}{E_1}\sigma_{x_1}^{\infty} = \frac{1}{E_2}\sigma_{x_2}^{\infty} \tag{14}$$

where $E_1 = 2G_1(1+v_1)$ and $E_2 = 2G_2(1+v_2)$ are Young's modulus of elasticity for upper and lower parts of bonded dissimilar materials, respectively.

The modified complex potentials (MCP) for the crack in the upper part of bonded dissimilar materials involve the principal parts $(\omega_{1p}(z),\phi_{1p}(z),\psi_{1p}(z))$ and the complementary parts $(\omega_{1c}(z),\phi_{1c}(z),\psi_{1c}(z))$ of the complex potentials defined as

$$\omega_1(z) = \omega_{1p}(z) + \omega_{1c}(z) \tag{15}$$

$$\phi_1(z) = \phi_{1p}(z) + \phi_{1c}(z) \tag{16}$$

$$\psi_1(z) = \psi_{1p}(z) + \psi_{1c}(z). \tag{17}$$

Whereas, for a crack in the lower part, the complex potentials are represented by $\omega_2(z)$, $\phi_2(z)$ and $\psi_2(z)$. The principal parts of complex potentials are referred to the complex potentials for the thermally insulated cracks in an infinite plane.

Since the temperature and resultant heat flux are continuous across the boundary, the heat conduction problem (1), yields

$$\left[\omega_1(t) + \overline{\omega_1(t)}\right]^+ = \left[\omega_2(t) + \overline{\omega_2(t)}\right]^-, \ t \in L \tag{18}$$

$$k_1\left[\omega_1(t) + \overline{\omega_1(t)}\right]^+ = k_2\left[\omega_2(t) + \overline{\omega_2(t)}\right]^-, \ t \in L \tag{19}$$

Applying Eqn. (15) into Eqns. (18) and (19), the following expressions are obtained

$$\begin{aligned}\omega_{1c}(z) &= \frac{k_1 - k_2}{k_1 + k_2}\overline{\omega_{1p}}(z),\ z \in S_1 + L_b,\\ \omega_2(z) &= \frac{2k_1}{k_1 + k_2}\omega_{1p}(z),\ z \in S_2 + L_b,\end{aligned} \tag{20}$$

where $\overline{\omega_{1p}}(z) = \overline{\omega_{1p}(\bar{z})}$, L_b is boundary of bonded dissimilar materials, S_1 and S_2 are upper and lower parts of bonded dissimilar materials, respectively. Whereas the continuity conditions for resultant force (3) and displacement (4) are defined as

$$\left[\phi_1(t) + t\overline{\phi_1'(t)} + \overline{\psi_1(t)}\right]^+ = \left[\phi_2(t) + t\overline{\phi_2'(t)} + \overline{\psi_2(t)}\right]^-, \tag{21}$$

$$\begin{aligned}&G_2\left[\kappa_1\phi_1(t) - t\overline{\phi_1'(t)} - \overline{\psi_1(t)} + (1+\kappa_1)G_1\beta_1\int\omega_1(t)dt\right]^+\\ &= G_1\left[\kappa_2\phi_2(t) - t\overline{\phi_2'(t)} - \overline{\psi_2(t)} + (1+\kappa_2)G_2\beta_2\int\omega_2(t)dt\right]^+\end{aligned} \tag{22}$$

where $t \in L$. Applying Eqns. (15), (16), (17) and (20) into Eqns. (21) and (22), the following expressions are obtained

$$\begin{aligned}\phi_{1c}(z) &= \frac{G_2 - G_1}{G_1 + \kappa_1 G_2}\left[z\overline{\phi'_{1p}}(z) + \overline{\psi_{1p}}(z)\right]\\ &+ \frac{(1+\kappa_1)G_1G_2\beta_1}{G_1 + \kappa_1 G_2}\frac{k_2 - k_1}{k_1 + k_2}\int_{L_1}\overline{\omega_{1p}}(z)dz,\ z \in S_1 + L_b\end{aligned} \tag{23}$$

$$\begin{aligned}\psi_{1c}(z) &= \frac{\kappa_1 G_2 - \kappa_2 G_1}{G_2 + \kappa_2 G_1}\overline{\phi_{1p}}(z) - z\phi'_{1c}(z)\\ &+ \frac{G_1G_2}{G_2 + \kappa_2 G_1}\left[(1+\kappa_1)\beta_1\int_{L_1}\overline{\omega_{1p}}(z)dz\right.\\ &\left.- \frac{2(1+\kappa_2)k_1\beta_2}{k_1 + k_2}\int_{L_2}\overline{\omega_{1p}}(z)dz\right],\ z \in S_1 + L_b\end{aligned} \tag{24}$$

$$\begin{aligned}\phi_2(z) &= \frac{(1+\kappa_1)G_2}{G_2 + \kappa_2 G_1}\phi_{1p}(z)\\ &+ \frac{G_1G_2}{G_2 + \kappa_2 G_1}\left[(1+\kappa_1)\beta_1\int_{L_1}\omega_{1p}(z)dz\right.\\ &\left.- \frac{2(1+\kappa_2)k_1\beta_2}{k_1 + k_2}\int_{L_2}\omega_{1p}(z)dz\right],\ z \in S_2 + L_b\end{aligned} \tag{25}$$

$$\begin{aligned}\psi_2(z) &= \frac{(1+\kappa_1)G_2}{G_1 + \kappa_1 G_2}\left[z\phi'_{1p}(z) + \psi_{1p}(z)\right] - z\phi'_2(z)\\ &+ \frac{(1+\kappa_1)G_1G_2\beta_1}{G_1 + \kappa_1 G_2}\frac{k_2 - k_1}{k_1 + k_2}\int_{L_1}\omega_{1p}(z)dz,\ z \in S_2 + L_b.\end{aligned} \tag{26}$$

The principal part of the traction for a thermally insulated crack in the upper part of bonded dissimilar materials can be obtained by substituting Eqns. (6) and (7) into (5) and letting point *z* approaches t_o on the crack. Changing $d\bar{z}/dz$ into $d\bar{t}_0/dt_0$, yields

$$\begin{aligned}\{N(t_0) + iT(t_0)\}_{1p} &= \frac{1}{\pi}\int_L\frac{g(t)dt}{(t-t_0)^2} + \frac{1}{2\pi}\int_L A_1(t,t_0)g(t)dt\\ &+ \frac{1}{2\pi}\int_L A_2(t,t_0)\overline{g(t)}dt\end{aligned} \tag{27}$$

where

$$A_1(t,t_0) = -\frac{1}{(t-t_0)^2} + \frac{1}{(\bar{t}-\bar{t}_0)^2}\frac{d\bar{t}}{dt}\frac{d\bar{t}_0}{dt_0},$$

$$A_2(t,t_0) = \frac{1}{(\bar{t}-\bar{t}_0)^3}\left(\frac{d\bar{t}}{dt} + \frac{d\bar{t}_0}{dt_0}\right) - \frac{2(t-t_0)}{(\bar{t}-\bar{t}_0)^3}\frac{d\bar{t}}{dt}\frac{d\bar{t}_0}{dt_0}$$

For the complementary part, substitutes Eqns. (23) and (24) into (5) and applying (6), (7) and (13), and letting point *z* approaches t_o on the crack and changing $d\bar{z}/dz$ into $d\bar{t}_0/dt_0$, yields

$$\{N(t_0)+iT(t_0)\}_{1c}=\frac{1}{2\pi}\int_L D_1(t,t_0)g(t)dt + \frac{1}{2\pi}\int_L D_2(t,t_0)\overline{g(t)}dt \tag{28}$$

$$D_1(t,t_0)=\frac{G_2-G_1}{G_1+\kappa_1 G_2}\Bigg[\left(\frac{1}{(t-\bar{t}_0)^2}+\frac{2(\bar{t}_0-\bar{t})}{(t-\bar{t}_0)^3}\right)+\left(\frac{1}{(t-\bar{t}_0)^2}+\frac{1}{(\bar{t}-t_0)^2}\right)\frac{d\bar{t}}{dt}$$
$$+\frac{d\bar{t}_0}{dt_0}\left(\frac{2(2t_0-3\bar{t}_0+\bar{t})}{(t-\bar{t}_0)^3}-\frac{6(\bar{t}_0-\bar{t})(\bar{t}_0-t_0)}{(t-\bar{t}_0)^3}-\frac{1}{(t-\bar{t}_0)^2}-\frac{d\bar{t}}{dt}\left(\frac{1}{(t-\bar{t}_0)^2}\right.\right.$$
$$\left.\left.+\frac{2(\bar{t}_0-t_0)}{(t-\bar{t}_0)^3}\right)\right)\Bigg]+\frac{\kappa_1 G_2-\kappa_2 G_1}{G_2+\kappa_2 G_1}\frac{d\bar{t}_0}{dt_0}\frac{1}{(t-\bar{t}_0)^2}$$
$$-\frac{1}{\beta_1}\Bigg[\frac{(1+\kappa_1)G_1G_2\beta_1}{G_1+\kappa_1 G_2}\frac{k_2-k_1}{k_1+k_2}\left(\frac{1}{t-\bar{t}_0}-\frac{d\bar{t}_0}{dt_0}\left(\frac{1}{t-\bar{t}_0}+\frac{\bar{t}_0-t_0}{(t-\bar{t}_0)^2}\right)\right)$$
$$+\frac{G_1G_2}{G_2+\kappa_2 G_1}\frac{d\bar{t}_0}{dt_0}\left(\frac{(1+\kappa_1)\beta_1}{t-\bar{t}_0}-\frac{2(1+\kappa_2)k_1\beta_2}{k_1+k_2}\frac{1}{t-\bar{t}_0}\right)\Bigg]$$

$$D_2(t,t_0)=\frac{G_2-G_1}{G_1+\kappa_1 G_2}\Bigg[\frac{1}{(\bar{t}-t_0)^2}+\frac{1}{(t-\bar{t}_0)^2}+\left(\frac{1}{(\bar{t}-t_0)^2}+\frac{2(t_0-t)}{(\bar{t}-t_0)^3}\right)\frac{d\bar{t}}{dt}$$
$$-\frac{d\bar{t}_0}{dt_0}\left(\frac{1}{(t-\bar{t}_0)^2}-\frac{2(t_0-\bar{t}_0)}{(t-\bar{t}_0)^2}\right)\Bigg]+\frac{(1+\kappa_1)G_1G_2\beta_1}{G_1+\kappa_1 G_2}\frac{k_2-k_1}{k_1+k_2}\frac{1}{\beta_1}\frac{1}{(t-\bar{t}_0)}\frac{d\bar{t}}{dt}$$

Summing Eqns. (27) and (28) yields the following HSIEs for a thermally insulated crack in the upper part of bonded dissimilar materials

$$\{N(t_0)+iT(t_0)\}_1=\{N(t_0)+iT(t_0)\}_{1p}+\{N(t_0)+iT(t_0)\}_{1c}$$
$$=\frac{1}{\pi}\int_L\frac{g(t)dt}{(t-t_0)^2}+\frac{1}{2\pi}\int_L E_1(t,t_0)g(t)dt+\frac{1}{2\pi}\int_L E_2(t,t_0)\overline{g(t)}dt \tag{29}$$

where

$$E_1(t,t_0)=A_1(t,t_0)+D_1(t,t_0),\quad E_2(t,t_0)=A_2(t,t_0)+D_2(t,t_0).$$

Note that the first integral in Eqn. (29) with the equal sign represent the hypersingular integral and must be defined as a finite part integral (Nik Long & Eshkuvatov, 2009). If $k_2=0$ and $G_2=0$ the Eqn. (29) reduce to the equation for a crack in half plane elasticity (Chen *et al.*, 2009). If $k_1=k_2$, $\mu_1=\mu_2$ and $G_1=G_2$ the Eqn. (29) reduce to the equation for a crack in an infinite plane (Rafar *et al.*, 2017).

For solving the HSIEs (29), the function $g(t)$ is mapped on a real axis s with an interval $2a$ as follows

$$g(t)\big|_{t=t(s)}=\sqrt{a^2-s^2}H(s), \tag{30}$$

where $H(s)=H_1(s)+iH_2(s)$. Then we apply the quadrature formulas introduced by Mayrhofer and Fischer (1992).

III. NUMERICAL RESULTS

Stress intensity factor (SIF) at the crack tips A_j is defined as

$$K_{A_j}=(K_1-iK_2)_{A_j}=\sqrt{2\pi}\lim_{t\to t_{A_j}}\sqrt{|t-t_{A_j}|}\,g'(t)=\sqrt{a\pi}F_{A_j} \tag{31}$$

where $j=1,2$ and $F_{A_j}=F_{1A_j}+iF_{2A_j}$ is the nondimensional SIF at cracks tips A_j. Note that in the sequel we denote G_2/G_1 the elastic constants ratio, k_2/k_1 heat conductivity ratio and μ_2/μ_1 thermal expansion coefficients ratio. Whereas for comparison purposes, we use $k_2/k_1=5.0$ and $\mu_2/\mu_1=1.0$ for crack with thermal, $k_1=k_2=0.0$ and $\mu_1=\mu_2=0.0$ for crack without thermal, and elastic constant ratio is $G_2/G_1=2.0$.

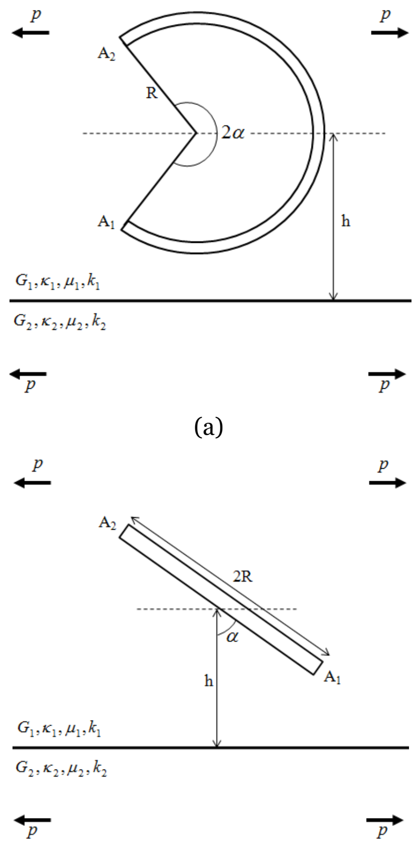

(a)

(b)

Figure 2. A thermally insulated crack in the upper part of bonded dissimilar materials

Consider a thermally insulated circular arc crack facing to the left (Figure 2(a)) and a thermally insulated inclined crack (Figure 2(b)) in the upper part of bonded dissimilar materials subjected to remote stress $\sigma_{x_1} = \sigma_{x_2} = p$.

Table 1 displays the nondimensional SIF for the problem defined in Figure 2(a) when $h = 2R$, $G_2/G_1 = 1.0$, $k_2/k_1 = 1.0$, $\mu_2/\mu_1 = 1.0$ and α varies. It is observed that F_1 at crack tip A_1 is equal to F_1 at crack tip A_2, whereas F_2 at crack tip A_1 is equal to the negative of F_2 at crack tip A_2. Our results are good agreement with those of Chen and Hasebe (2003).

Table 1. SIF for a thermally insulated circular arc crack when $h = 2R$, $G_2/G_1 = 1.0$, $k_2/k_1 = 1.0$, $\mu_2/\mu_1 = 1.0$ and α varies

SIF	α								
	10°	20°	30°	40°	50°	60°	70°	80°	90°
F_{1A1}*	0.9735	0.8970	0.7783	0.6278	0.4583	0.2823	0.1115	-0.0441	-0.1764
F_{1A1}**	0.9736	0.8970	0.7779	0.6272	0.4575	0.2815	0.1107	-0.0447	-0.1768
F_{2A1}*	01727	0.3317	0.4672	0.5704	0.6362	0.6630	0.6516	0.6057	0.5306
F_{2A1}**	01723	0.3318	0.4673	0.5703	0.6359	0.6625	0.6511	0.6053	0.5303

* Current study

** (Chen & Hasebe, 2003)

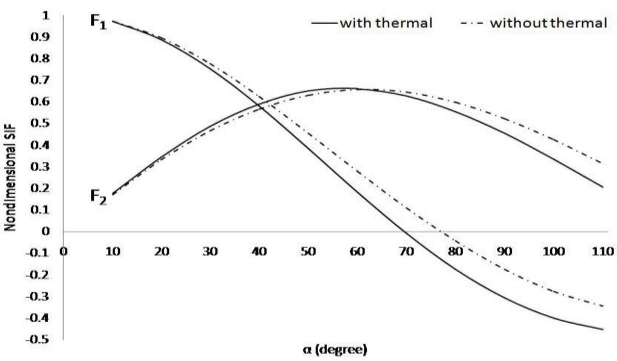

(a)

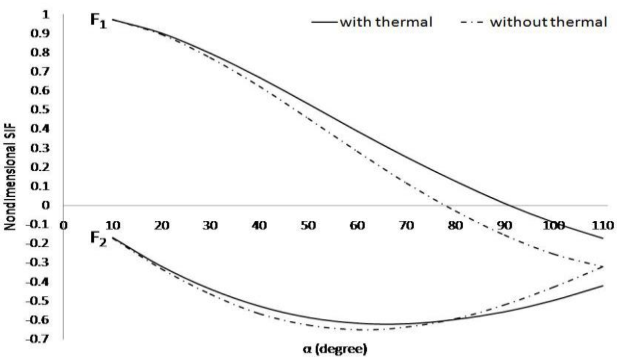

(b)

Figure 3. Comparison of the nondimensional SIF with and without thermal when $h = 2R$ and α varies (Figure 2(a))

Figure 3 shows the comparison between the nondimensional SIF at crack tips A_1 and A_2 with and without thermal when $h = 2R$ and α varies for the problem defined in Figure 2(a). It is found that at crack tip A_1, F_1 and F_2 for the crack without thermal is higher than F_1 and F_2 for the crack with thermal. While at crack tip A_2, F_1 for the crack without thermal is lower than F_1 for the crack with thermal, however F_2 for the crack without thermal is higher than F_2 for the crack with thermal for $\alpha > 80^o$. For different values of G_2/G_1 when $\mu_2/\mu_1 = 0.5$, $k_2/k_1 = 2.0$, $h = 2R$ and α varies the nondimensional SIF at crack tips A_1 and A_2 are presented in Figure 4. It is found that at crack tip A_1, as α increases F_1 decreases and F_2 decreases for $\alpha > 60^o$, and as G_2/G_1 increases F_1 and F_2 decrease. Whereas at crack tip A_2, as α increases F_1 decreases and F_2 decreases for $\alpha < 60^o$, and as G_2/G_1 increases F_1 increases and F_2 increases for $\alpha < 90^o$. For different values of k_2/k_1 when $G_2/G_1 = 0.5$, $\mu_2/\mu_1 = 2.0$, $h = 2R$ and α varies the nondimensional SIF at crack tips A_1 and A_2 are presented in Figure 5. It is observed that at crack tip A_1, as α increases F_1 decreases and F_2 decreases for $\alpha > 60^o$, and as k_2/k_1 increases F_1 decreases and F_2 increases. Whereas at crack tip A_2, as α increases F_1 decreases and F_2 decreases for $\alpha < 50^o$, and as k_2/k_1 increases F_1 increases and F_2 decreases for $\alpha > 50^o$. For different values of μ_2/μ_1 when $k_2/k_1 = 0.5$, $G_2/G_1 = 2.0$, $h = 2R$ and α varies the nondimensional SIF at crack tips A_1 and A_2 are presented in Figure 6. It is found that at crack tip A_1, as α increases F_1 decreases and F_2 does not show any significant for

$\mu_2/\mu_1 = 5.0$ and for other values of μ_2/μ_1 F_2 increases when $\alpha < 60^o$, and as μ_2/μ_1 increases F_1 increases and F_2 decreases. Whereas at crack tip A_2, for $\mu_2/\mu_1 = 5.0$ F_1 increases when $\alpha > 60^o$ and F_2 increases when $\alpha > 30^o$, for other values of μ_2/μ_1 F_1 decreases as α increases and F_2 decreases for $\alpha < 50^o$, and as μ_2/μ_1 increases F_1 decreases and F_2 increases.

Figure 7 presents the comparison between the nondimensional SIF at all crack tips in bonded dissimilar materials with and without thermal when $R/h = 0.9$ and α varies for the problem defined in Figure 2(b). It is observed that F_1 for the crack without thermal is higher than F_1 for the crack with thermal at all crack tips, while F_2 for the crack without thermal is lower than F_2 for the crack with thermal.

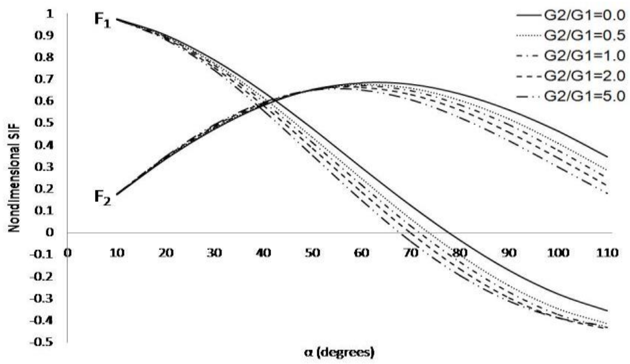

(a)

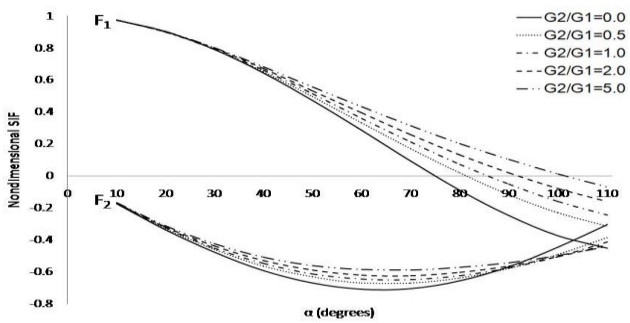

(b)

Figure 4. Nondimensional SIF for different values of G_2/G_1 when $\mu_2/\mu_1 = 0.5$, $k_2/k_1 = 2.0$, $h = 2R$ and α varies (Figure 2(a))

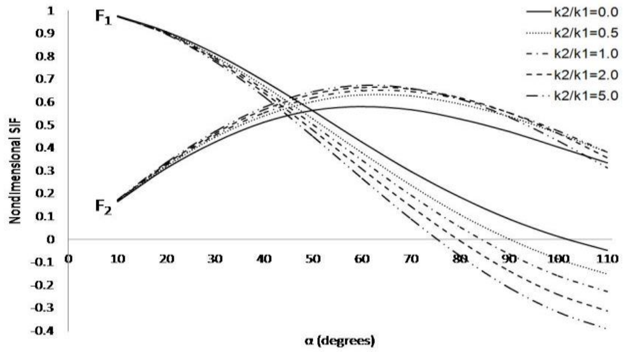

(a)

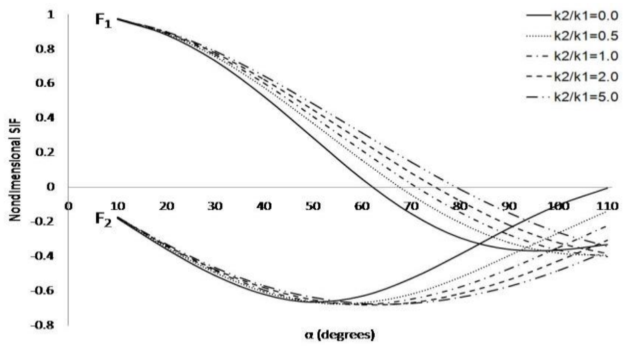

(b)

Figure 5. Nondimensional SIF for different values of k_2/k_1 when $G_2/G_1 = 0.5$, $\mu_2/\mu_1 = 2.0$, $h = 2R$ and α varies (Figure 2(a))

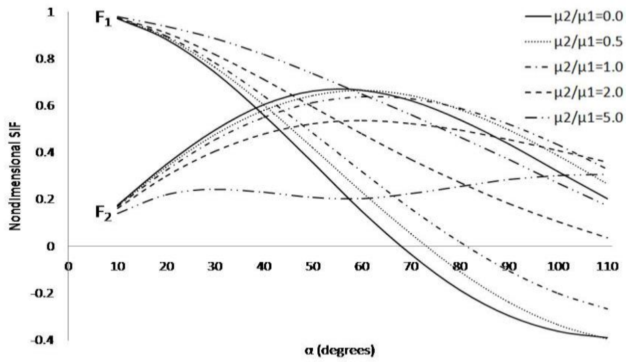

(a)

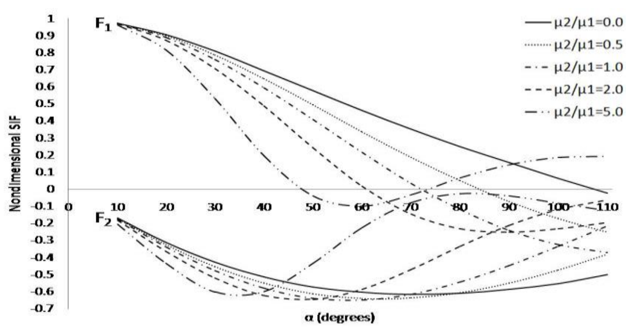

(b)

Figure 6. Nondimensional SIF for different values of μ_2/μ_1 when $k_2/k_1 = 0.5$, $G_2/G_1 = 2.0$, $h = 2R$ and α varies (Figure 2(a))

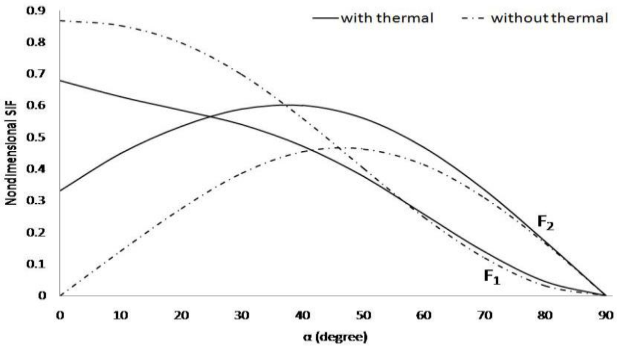

(a)

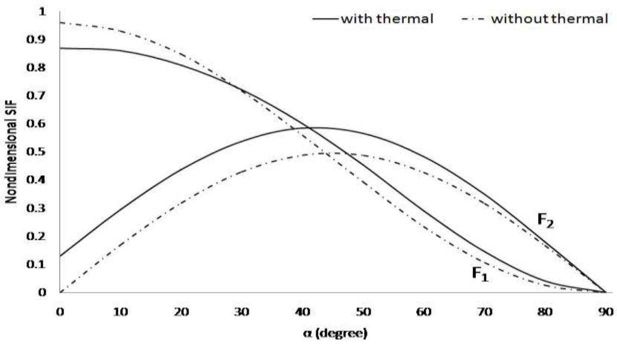

(b)

Figure 7. Comparison of the nondimensional SIF with and without thermal versus α when $R/h = 0.9$ (Figure 2(b))

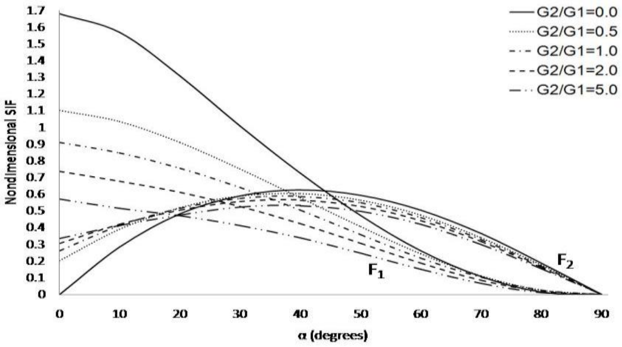

(a)

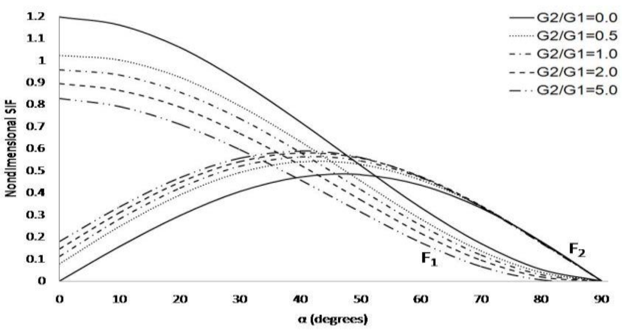

(b)

Figure 8. Nondimensional SIF for different values of G_2/G_1 when $\mu_2/\mu_1 = 0.5$, $k_2/k_1 = 2.0$, $R/h = 0.9$ and α varies (Figure 2(b))

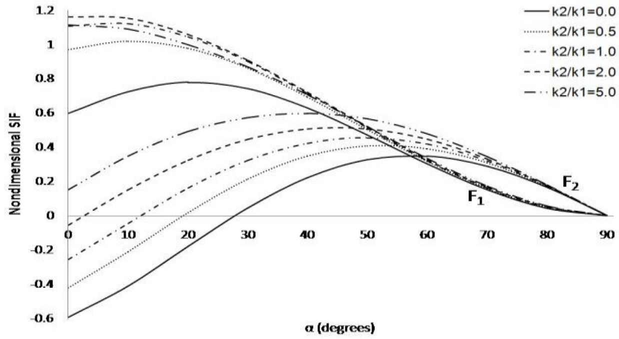

(a)

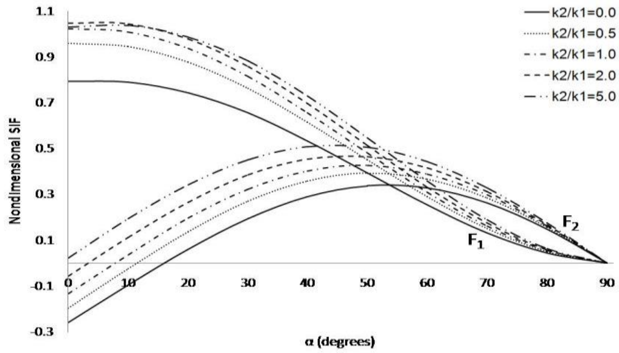

(b)

Figure 9. Nondimensional SIF for different values of k_2/k_1 when $G_2/G_1 = 0.5$, $\mu_2/\mu_1 = 2.0$, $R/h = 0.9$ and α varies (Figure 2(b))

Figure 8 presents the nondimensional SIF for different values of G_2/G_1 when $\mu_2/\mu_1 = 0.5$, $k_2/k_1 = 2.0$, $R/h = 0.9$ and α varies (Figure 2(b)). It is found that at crack tip A_1, as α increases F_1 decreases and F_2 decreases for $\alpha > 45^o$, and as G_2/G_1 increases F_1 decreases and F_2 decreases for $\alpha > 25^o$. Whereas at crack tip A_2, F_1 behaves as F_1 at crack tip A_1, while F_2 increases for $\alpha < 45^o$ and as G_2/G_1 increases. Figure 9 presents the nondimensional SIF for different values of k_2/k_1 when $G_2/G_1 = 0.5$, $\mu_2/\mu_1 = 2.0$, $R/h = 0.9$ and α varies (Figure 2(b)). It is found that F_1 decreases for $\alpha > 20^o$ and F_2 increases for $\alpha < 50^o$ at all crack tips. Whereas F_1 and F_2 increase at all crack tips as G_2/G_1 increases.

IV. CONCLUSION

In this paper, the HSIE for a thermally insulated crack problems in the upper part of bonded dissimilar materials is formulated by using the modified complex variable function method with the COD function as the unknown.

The HSIE reduces to a crack problem in a half plane when $k_2 = 0$ and $G_2 = 0$, and for $k_1 = k_2$, $\mu_1 = \mu_2$ and $G_1 = G_2$ the HSIE reduce to a crack problem in an infinite plane. The Mode I and Mode II nondimensional SIF at the crack tips depends on the elastic constant ratio G_2/G_1, heat conductivity ratio k_2/k_1, thermal expansion coefficients ratio μ_2/μ_1 and cracks geometries. The nondimensional SIF at crack tips for a crack without thermal is higher than nondimensional SIF for a crack with thermal, however the position and crack geometries play an important role to the behaviour of nondimensional SIF.

V. ACKNOWLEDGEMENT

The first author would like to thank to the Ministry of Education Malaysia, Universiti Putra Malaysia and Universiti Teknikal Malaysia Melaka for the financial support. The second author would like to thank the Universiti Putra Malaysia for Putra Grant, project no: 9567900 and Fundamental Research Grant Scheme (FRGS) project no: 01-01-16-18685R5524975.

VI. REFEREENCES

Chao, CK & Shen, MH 1995, 'Solutions of thermoelastic crack problems in bonded dissimilar media or half-plane medium', International Journal of Solids Structures, vol. 32, no. 24, pp. 3537-3554.

Chen, YZ & Hasebe, N 2003, 'Solution for a Curvilinear Crack in a Thermoelastic Medium', Journal of Thermal Stresses, vol. 26, no. 3, pp. 245-259.

Chen, YZ, Hasebe, N & Lee, KY 2003, *Multiple crack problems in elasticity*, WIT Press, Southampton.

Chen, YZ, Lin, XY & Wang, XZ 2009, 'Numerical solution for curved crack problem in elastic half-plane using hypersingular integral equation', Philosophical Magazine, vol. 89, no. 26, pp. 2239-2253.

Choi, HJ 2016, 'Analysis of Stress Intensity Factors for Edge Interfacial Cracks in Bonded Dissimilar Media with a Functionally Graded Interlayer under Antiplane Deformation', Theoretical and Applied Fracture Mechanics, vol. 82, pp. 88-95.

Ding, SH & Li, X 2015, 'Thermoelastic analysis of nonhomogeneous structural materials with an interface crack under uniform heat flow', Applied Mathematics and Computation, vol. 271, pp. 22-33.

Jin, ZH & Noda, N 1993, 'An internal crack parallel to the boundary of a nonhomogeneous half plane under thermal loading', International Journal of Engineering Science, vol. 31, no. 5, pp. 793-806.

Li, W, Li, J, Abdelmoula, R, Song, F & Jiang, CP 2015, 'Inertia effect analysis of a half-plane with an induced crack under thermal loading using hyperbolic heat conduction', Journal of Applied Mathematics and Mechanics, pp. 1-17.

Mayrhofer, K & Fischer, FD 1992, 'Derivation of a new analytical solution for a general two-dimensional finite-part integral applicable in fracture mechanics', International Journal of Numerical Method in Engineering, vol. 33, no. 5, pp. 1027-1047.

Mishra, PK & Das, S 2018, 'Two interfacial collinear griffith cracks in thermo-elastic composite media', Thermal Science, vol. 22, no. 1B, pp. 423-433.

Muskhelishvili, NI 1953, *Some basic problems of the mathematical theory of elasticity*, Noordhoff International Publishing, Leyden.

Nik Long, NMA & Eshkuvatov ZK 2009, 'Hypersingular integral equation for multiple curved cracks problem in plane elasticity', International Journal of Solids and Structures, vol. 46, pp. 2611-2617.

Rafar, RA, Nik Long, NMA, Senu, N & Noda, NA 2017, 'Stress intensity factor for multiple inclined or curved cracks problem in circular positions in plane elasticity', Journal of Applied Mathematics and Mechanics, vol. 97, pp. 1482-1495.

Shevchuk, VA 2017, 'Thermoelasticity problem for a multilayer coating/half-space assembly with undercoat crack subjected to convective thermal loading', Journal of Thermal Stresses, vol. 40, no. 10, pp. 1215-1230.

Shields, EB, Srivatsan, TS & Padovan J 1992, 'Analytical methods for evaluation of stress intensity factors and fatigue crack growth', Engineering Fracture Mechanics, vol. 42, no. 1, pp. 1-26.

Zhong, XC, Long, XY & Zhang, LH 2018, 'An extended thermal-medium crack model', Applied Mathematical Modelling, vol. 56, pp. 202-216.

Zhou, YT & Kim, TW 2016, 'Thermal resistance inside an interface crack in the functionally graded sandwich structures', Fatigue and Fracture of Engineering Materials and Structures, vol. 39, pp. 1067-1081.